Detecting nonmagnetic excitations in quantum magnets

Zhihao Hao

Department of Physics and Astronomy, Johns Hopkins University, Baltimore, Maryland 21218, USA and
Department of Physics and Astronomy, University of Waterloo, Waterloo, Ontario N2L 3G1, Canada

(Received 25 October 2011; published 25 May 2012)

Many unconventional quantum phases host special nonmagnetic excitations such as photons and visons. We discuss two possible ways to detect these excitations experimentally. First, spin-lattice coupling mixes the excitations with phonons. The phonon spectral function acquires new features that can be detected by neutron or x-ray scattering. Second, valence-bond fluctuations translate into charge density fluctuations on nonbipartite lattices. Such charge fluctuations can be characterized by conventional spectroscopies such as terahertz spectroscopy. As by-products, we discuss the general mechanisms of spin-Peierls transitions in two- and three-dimensional spin liquids.

DOI: 10.1103/PhysRevB.85.174432 PACS number(s): 75.10.Jm, 75.10.Kt

I. INTRODUCTION

The search for exotic quantum phases[1] in frustrated antiferromagnets has been one of the main challenges in the field of strongly correlated systems. Such phases are believed to emerge when long-range order is destroyed by competing interactions and strong quantum fluctuations. In a typical situation, SU(2) symmetry remains intact down to zero temperature so that excitations can be classified by their spin. While magnetic excitations can be studied using techniques such as inelastic neutron scattering (i.e., spinons),[2,3] exotic nonmagnetic excitations remain elusive.

Indeed, novel nonmagnetic excitations are predicted in generic unconventional magnetic phases. Consider the seminal resonating valence-bond (RVB) phase.[4] Extensive investigations of the quantum dimer model (QDM)[1] revealed that there are two types of dimer liquids in two and three dimensions. The $U(1)$ liquid exists on bipartite lattices in three dimensions. Its low-energy excitations are transverse gapless fluctuations of dimer density, or "photons" of an emergent $U(1)$ gauge theory.[5] On the other hand, the Z_2 liquid appears in nonbipartite lattices and possesses topological order. The low-energy excitations are Z_2 vortices, or "visons."[6,7] While a single vison is a nonlocal object, excitations of an even number of visons correspond to dimer density fluctuations.[8,9]

While these results were obtained in the QDM, generic constructions[10,11] exist in which QDMs are low-energy limits of SU(2) invariant spin models. Such phases and excitations could exist in the low-energy limits of the Heisenberg model thanks to universality. The authors of an extensive density-matrix renormalization group (DMRG)[12] study of a spin-1/2 Heisenberg antiferromagnetic model on the kagome lattice concluded that its ground state is a Z_2 spin liquid. Studies of the multispin exchange model[13,14] on a triangular lattice found a gapped spin-liquid phase that looks like a Z_2 liquid. Both models are realized in real materials (for reviews, see Refs. 1 and 15). Observing singlet excitations in these materials would be positive evidence of the existence of the Z_2 liquid phase in nature.

In this paper, we discuss two general ways to experimentally probe singlet excitations in quantum antiferromagnets. First, singlet excitations mix with optical phonons through spin-lattice coupling. For suitable parameters, this leads to new features in the phonon spectral function which can be detected by neutron or x-ray scattering. Spin-lattice coupling has been an exciting topic throughout the years. Its study was pioneered by the discovery and characterization of the spin-Peierls transition.[16–19] It was realized[20,21] that similar mechanisms can induce long-range order in the highly frustrated Heisenberg antiferromagnet on the pyrochlore lattice. Magnetoelastic splitting of degenerate optical phonons was observed in $ZnCr_2O_4$ (Ref. 22) and a number of other compounds. The strongest effect (10% splitting) has been seen in MnO.[23] Wang and Vishwanath generalized the idea to a local phonon.[24] The dynamical effects of phonons were explored,[25] motivated by the spin-Peirels compound $CuGeO_3$ (Refs. 26 and 27). These studies demonstrated the importance of both the static and dynamical effects of the spin-lattice coupling.

The second way exploits the ability of singlet excitations to couple directly to an electric field. Bulaevskii *et al.*[28] discovered that some magnetic ground states and excitations of certain Mott insulators have nonzero local electric charge or current. In particular, fluctuations of valence-bond densities induces electric dipoles. The coupling is stronger for weak Mott insulators due to smaller U/t, where t is the hopping amplitude of electrons and U is the onsite repulsion. Spin-lattice coupling can lead to the same effect.[28] Consequently, valence-bond density fluctuations couple to electromagnetic radiations directly. Conventional spectroscopic techniques may be used to directly detect nonmagnetic excitations.

The rest of the paper is organized as follows. First, we study the mixing between optical phonons and singlet excitations. We introduce the general formulation of the mixing and summarize the main results in Sec. II. The formulation is applied to both $U(1)$ and Z_2 liquids in Secs. III and IV. In these sections, we also discuss the general mechanisms of spin-Peierls transitions in both liquids. We then illustrate in Sec. V the possible charge signature of singlet excitations in the context of the spin-1/2 Heisenberg antiferromagnetic model on kagome. Finally, we conclude our paper by discussing possible discoveries of singlet excitations in real materials.

II. GENERAL FORMULATION

Let us demonstrate the first mechanism in the simplest context. Consider spins interacting via Heisenberg exchange

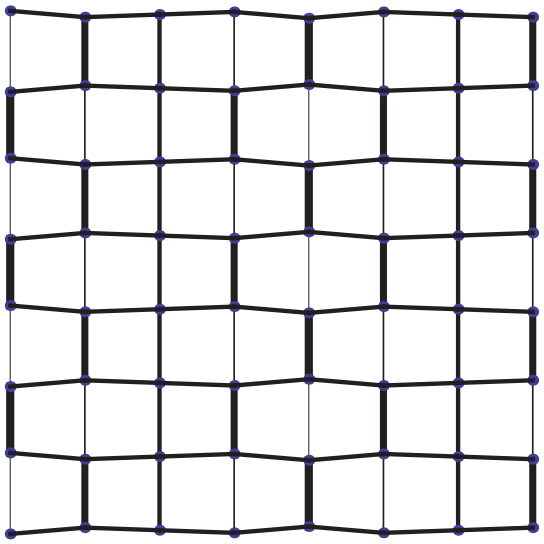

FIG. 1. (Color online) The new phonon mode around $\mathbf{Q}$ is illustrated on a two-dimensional slice of cubic lattice. The mode is induced by the "photon," i.e., transverse fluctuation of dimer densities. Bond thicknesses reflect dimer densities.

whose strength depends on the distance between the spins:[20–22]

$$J(R+u)\mathbf{S}_i\cdot\mathbf{S}_j \approx J(R)\mathbf{S}_i\cdot\mathbf{S}_j + \left.\frac{\partial J}{\partial r}\right|_{r=R}(\mathbf{S}_i\cdot\mathbf{S}_j)u. \quad (1)$$

Here, R is the equilibrium distance between the two spins if there is no spin-lattice coupling. u is the elongation of the bond, and u couples linearly with bond operator $\mathbf{S}_i\cdot\mathbf{S}_j$ which measures the singlet density on bond $\langle ij\rangle$. The coupling mixes the singlet excitations and phonons. The phonon spectral function will acquire features of the singlet excitations.

To elaborate on this idea, we consider the following Hamiltonian on a general lattice:

$$H=\sum_{\mathbf{r}}\left[\frac{1}{2}\dot{\mathbf{u}}(\mathbf{r})^2+\frac{1}{2}\omega_0^2\mathbf{u}(\mathbf{r})^2+f\mathbf{u}(\mathbf{r})\cdot\mathbf{V}(\mathbf{r})\right]+H_s. \quad (2)$$

Here, H_s is the spin Hamiltonian and $\mathbf{u}(\mathbf{r})$ is the displacement of the ion at site $\mathbf{r}$. We adopt the Einstein phonon model with mass of the ion assumed to be 1 for simplicity. Based on the model in Eq. (1), the $\mathbf{V}(\mathbf{r})$ field is defined as follows:[24]

$$\mathbf{V}(\mathbf{r})=\frac{1}{f}\sum_{\mathbf{r}'\in\{\mathbf{r}\}}\hat{e}_{\mathbf{r}\mathbf{r}'}[\hat{e}_{\mathbf{r}\mathbf{r}'}\cdot\nabla_{\mathbf{r}}J(\mathbf{r}-\mathbf{r}')]\mathbf{S}_{\mathbf{r}}\cdot\mathbf{S}_{\mathbf{r}'}. \quad (3)$$

Here, $\{\mathbf{r}\}$ is the set of neighbors of site $\mathbf{r}$ and $\hat{e}_{\mathbf{r}\mathbf{r}'}\equiv(\mathbf{r}-\mathbf{r}')/|\mathbf{r}-\mathbf{r}'|$. $f=\sum_{\mathbf{r}'\in\{\mathbf{r}\}}\hat{e}_{\mathbf{r}\mathbf{r}'}\cdot\nabla_{\mathbf{r}}J_{\mathbf{r}-\mathbf{r}'}$ is the spin-lattice coupling.

For small ion displacements, the full phonon Green's function in the random-phase approximation (RPA) is

$$\tilde{G}^{-1}_{\alpha\beta}(\mathbf{r}_1,t_1;\mathbf{r}_2,t_2)=G^{-1}_{\alpha\beta}(\mathbf{r}_1,t_1;\mathbf{r}_2,t_2)-f^2\chi_{\alpha\beta}(\mathbf{r}_1,t_1;\mathbf{r}_2,t_2), \quad (4)$$

where $\tilde{G}$ is the full phonon Green's function, G is the bare one, and χ is the time-ordered bond-bond correlation function,

$$\chi_{\alpha\beta}(\mathbf{r}_1,t_1;\mathbf{r}_2,t_2)\equiv\langle \mathrm{T}\{V_\alpha(\mathbf{r}_1,t_1)V_\beta(\mathbf{r}_2,t_2)\}\rangle. \quad (5)$$

In the Fourier space, relation (4) is written as

$$\tilde{G}^{-1}_{\alpha\beta}(\mathbf{k},\omega)=G^{-1}_{\alpha\beta}(\mathbf{k},\omega)-f^2\chi_{\alpha\beta}(\mathbf{k},\omega). \quad (6)$$

In Secs. III and IV, we will explore the consequence of Eqs. (4) and (6). For readers not interested in technical details, we summarize the main results here. These readers can continue directly to Sec. VI .

There are two types of dimer liquids.[1] The $U(1)$ dimer liquid exists on three-dimensional bipartite lattices.[1,5] Its low-energy effective theory has the same form as electrodynamics.[5] The magnetic field $\mathbf{B}$ is related to the dimer, or singlet, density. Low-energy excitations, i.e., photons,[5] are transverse fluctuations of the singlet density. The mixture between optical phonons and photons generates new transverse sound modes. In contrast to acoustic phonons, there is no longitudinal mode. For a cubic lattice, the new sound modes are located at momentum $Q=(\pi,\pi,\pi)$. Such modes can be observed experimentally using x-ray or neutron-scattering techniques. If the spin-lattice coupling is larger than a critical value, then the velocity of the new sound modes becomes negative. The system enters a valence-bond solid phase and the lattice distorts. The two transverse sound modes become the fluctuations of the magnitude and the direction of the condensate, respectively. The fluctuation of the magnitude is gapless and disperses along only one direction. On the other hand, the direction fluctuation of the lattice distortion and singlet condensate are constrained to be perpendicular to each other.

The Z_2 liquid phase is the ground state of QDMs on two- and three-dimensional nonbipartite lattices.[1] The phase preserves all symmetries and is gapped to all excitations. It possesses topological order:[1] the degree of degeneracy of the ground state depends on the topology of the hosting manifold. The low-energy theory is the Z_2 gauge theory.[1,29] Elementary excitations are visons,[6,7] i.e., massive bosonic particles. The visons are nonlocal excitations; singlet density fluctuations involve at least two visons.[8,9] Vison dispersion can be determined by the Z_2 gauge theory.[1,29] The coupling between one phonon and two visons induces new phonon modes below the edge of the two-vison continuum. As the vison mass decreases, these new phonon modes move away from the continuum and gain spectrum density. For suitable parameters, such modes can be observed by x-ray and neutron scattering. We stress that the Z_2 gauge theory *predicts* the momentum and the relative strength of these new modes. They provide specific signatures of the Z_2 liquid phase that can be verified or falsified by experiments. As the vison mass becomes smaller than a critical value, one or several new phonon modes condense and the system becomes a valence-bond solid. This is the general mechanism of the spin-Peirels transition in the Z_2 liquid phase.

III. $U(1)$ LIQUID

The first type of spin liquid is the $U(1)$ liquid. Such liquid is the ground state of QDMs on three-dimensional bipartite lattices for an extended parameter region. As an example, we focus on the QDM on a cubic lattice. The QDM on a cubic lattice has two phases:[5] the staggered valence-bond crystal phase and the $U(1)$ liquid phase. The low-energy physics of the liquid phase is described by the following Hamiltonian in

the continuum limit:[5]

$$H_s = \int d^3r \left[\frac{1}{2}\mathbf{E}^2 + \frac{1}{2}\rho_2\mathbf{B}^2 + \rho_4(\nabla\times\mathbf{B})^2\right]. \quad (7)$$

In the Coulomb gauge $A_0 = 0$, $\nabla\cdot\mathbf{A} = 0$, the electric and magnetic fields are expressed as $\mathbf{E} = \partial_t\mathbf{A}$ and $\mathbf{B} = \nabla\times\mathbf{A}$. On the lattice, the magnetic field $\mathbf{B}$ is defined on the bonds:[30]

$$B_\alpha(\mathbf{r}) = e^{i\mathbf{Q}\cdot\mathbf{r}}\left(n_\alpha(\mathbf{r}) - \frac{1}{z}\right), \quad (8)$$

where $\mathbf{Q} = (\pi,\pi,\pi)$ and $n_\alpha(\mathbf{r})$ is the number of dimers on the bond connecting $\mathbf{r}$ and $\mathbf{r}+\hat{\alpha}$ ($\alpha = x,y,z$). Here, $z = 6$ is the coordination number of the cubic lattice.

To include the spin-lattice coupling, we write the bond operator $\mathbf{S}(\mathbf{r})\cdot\mathbf{S}(\mathbf{r}+\hat{\alpha})$ in terms of the gauge field. The bond operator amounts to two operations on a general dimer covering. Its diagonal part counts the number of dimers on the bond, while the off-diagonal part flips the dimers around the plaquette to which the bond belongs. The plaquette-flipping operator translates into $\mathbf{E}^2$.[5] As a result, the off-diagonal term is irrelevant in the renormalization-group sense. The spin-lattice Hamiltonian translates into the following compact form in the continuum limit:

$$H_{sp} = \int d^3r f_1\mathbf{B}\cdot\tilde{\mathbf{u}}, \quad (9)$$

where $\tilde{\mathbf{u}} \equiv e^{i\mathbf{Q}\cdot\mathbf{r}}\mathbf{u}$ and f_1 is the spin-lattice coupling. The Hamiltonian for the phonon is

$$H_p = \int d^3r \left[\frac{1}{2}(\partial_t\tilde{\mathbf{u}})^2 + \frac{1}{2}\omega_0^2\tilde{\mathbf{u}}^2\right]. \quad (10)$$

The total Hamiltonian is $H = H_p + H_{sp} + H_s$.

We focus on the phonon spectrum in the $U(1)$ liquid phase where the ρ_4 term can be neglected. Applying Eqs. (4) and (6), the phonon develops two transverse sound modes around momentum $\mathbf{Q}$ (see supplementary meterial[31]). These modes manifest themselves as new low-energy poles in the phonon spectral function. For momentum $\mathbf{Q}+\mathbf{k}$ ($k \ll 1$), the energy is approximately

$$\omega(\mathbf{k}) \approx \sqrt{\rho_2 - \frac{f_1^2}{\omega_0^2}}k. \quad (11)$$

The spectrum weight of the modes is proportional to $f_1^2k^2/(\omega_0^2 - \rho_2k^2)^2$. In contrast, the spectrum of the longitudinal phonon remains unchanged. This is a reflection of the transverse nature of gauge fluctuations. Such sound modes generally exist in QDMs on other three-dimensional bipartite lattices.

If $f_1 > \omega_0\sqrt{\rho_2}$, then these sound modes become unstable. The system develops a valence-bond order at momentum $\mathbf{Q}$ and the lattice distorts accordingly. This is the spin-Peierls transition in the three-dimensional $U(1)$ liquid. To understand this transition better, we write out the "potential energy" as a function of $\tilde{\mathbf{u}}$ and $\mathbf{B}$:

$$V(\tilde{\mathbf{u}},\mathbf{B}) = \tfrac{1}{2}\omega_0^2\tilde{\mathbf{u}}^2 + f_1\tilde{\mathbf{u}}\cdot\mathbf{B} + \tfrac{1}{2}\rho_2\mathbf{B}^2. \quad (12)$$

We write both the $\tilde{\mathbf{u}}$ and $\mathbf{B}$ in terms of a parallel component and a perpendicular component:

$$\tilde{\mathbf{u}} = u\hat{z} + \mathbf{u}_\perp, \quad \mathbf{B} = -B\hat{z} + \mathbf{B}_\perp, \quad (13)$$

where $\mathbf{u}_\perp\cdot\hat{z} = 0$, $\mathbf{B}_\perp\cdot\hat{z} = 0$, and $\mathbf{u}_\perp\cdot\mathbf{B}_\perp = 0$. The potential energy V also splits into the "parallel" part $V_\parallel$ and the "perpendicular" part $V_\perp$ under the parametrization.

We consider the parallel part first:

$$V_\parallel = \tfrac{1}{2}\omega_0^2u^2 - f_1uB + \tfrac{1}{2}\rho_2B^2. \quad (14)$$

It can be rewritten in terms of normal models $\eta_1 \equiv \cos(\theta/2)u - \sin(\theta/2)B$ and $\eta_2 \equiv \sin(\theta/2)u + \cos(\theta/2)B$ with $\theta \equiv \tan^{-1}[2f_1/(\omega_0^2 - \rho_2)]$:

$$V_\parallel = \tfrac{1}{2}\left(\lambda_1\eta_1^2 + \lambda_2\eta_2^2\right) + K_1\eta_1^4 + K_2\eta_2^4, \quad (15)$$

where $\lambda_{1,2} = 1/2(\omega_0^2+\rho_2) \pm \sqrt{1/4(\omega_0^2-\rho_2)^2 + f_1^2}$ and $K_{1,2} > 0$. The quartic terms are added to ensure the stability. Physically, they come from the anharmonic contributions in phonon energy. When $f_1 > \omega_0\sqrt{\rho_2}$, λ_2 becomes negative and the η_2 mode condenses. The magnitude of the condensate is proportional to $f_1 - \omega_0\sqrt{\rho_2}$.

In the condensed phase, both the magnitude and the direction of the condensate fluctuate. To study the magnitude fluctuations, we rewrite $u = \bar{u} + \delta u$ and $B = \bar{B} + \delta B$ in Eq. (14) and keep only the quadratic terms in δu and δB. We introduce $\delta\mathbf{A}$ such that $\nabla\times\delta\mathbf{A} = \delta B\hat{z}$. The gauge is fixed by demanding $\delta\mathbf{A} = \delta A\hat{y}$ so that $\partial_x\delta A = \delta B$. After standard manipulations, we discover that the magnitude fluctuation has a low-energy mode with the following dispersion:

$$\omega^2 \approx \frac{4\sqrt{\rho_2}}{\omega_0}(f_1 - \omega_0\sqrt{\rho_2})k_x^2. \quad (16)$$

This mode is gapless and only disperses along one direction. Just as in the liquid phase, the mode can be observed by scattering techniques since it is a mixture of phonon and dimer density fluctuation.

The fluctuation of the condensate direction is controlled by $V_\perp$:

$$V_\perp = \tfrac{1}{2}\omega_0^2\mathbf{u}_\perp^2 + \tfrac{1}{2}\rho_2\mathbf{B}_\perp^2. \quad (17)$$

Naively, it seems that $\mathbf{u}_\perp$ and $\mathbf{B}_\perp$ are effectively decoupled. However, their directions are strongly correlated by the constraint that $\mathbf{u}_\perp\cdot\mathbf{B}_\perp = 0$.

These results are expected from general arguments. The condensation of normal mode η_2 defines a special direction. As a result, the degeneracy between the two transverse low-energy modes in the liquid phase is lifted. These two modes become the magnitude and the direction fluctuations, respectively. While the ordering wave vector of the condensed phase depends on the lattice, the mechanisms described above are generally applicable to all three-dimensional bipartite lattices.

IV. Z_2 LIQUID PHASE

The second generic dimer liquid phase is the Z_2 liquid phase on two- and three-dimensional nonbipartite lattices.[1] Such a state preserves all lattice symmetries and has a gap to all excitations. The system possesses topological order. Consider a Z_2 liquid on a cylinder; the state belongs to the even or odd topological sectors if a cut around the cylinder crosses an even or odd number of dimers. The low-energy excitations are visons,[6,7] i.e., Z_2 vortices residing on the sites of the dual lattices. At the Rokhsar-Kivelson (RK)[32] point, the ground state is an equal amplitude combination of all possible dimer

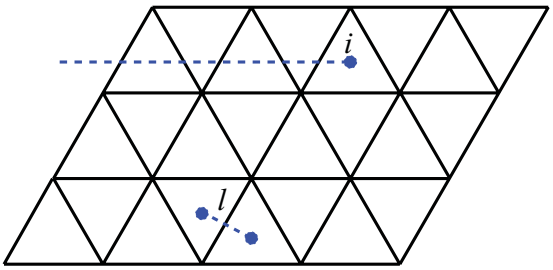

FIG. 2. (Color online) One-vison and two-vison excitations. A vison at i is created by operators on all of the bonds to the left of i. A two-vison excitation is related to the dimer density on the bond l between them.

states. To obtain a vison at site $\tilde{\mathbf{r}}$, we make a cut[1] from the site to the lattice boundary (Fig. 2). A state with one vison is a combination of all possible dimer coverings. However, the amplitude of a dimer covering is negative if the cut crosses an odd number of dimers. Visons are nonlocal objects. A local operator such as $\mathbf{S}_{\mathbf{r}} \cdot \mathbf{S}_{\mathbf{r}+\hat{l}}$ involves an even number of visons.

In the remainder of the section, we describe how phonons are coupled to visons through spin-lattice coupling using the Z_2 liquid phase on the triangular lattice as an example. First, we briefly review the Z_2 gauge theory description of the liquid phase. The vison-phonon coupling is derived both from microscopic models and through symmetry arguments. Under the RPA approximation, the coupling introduces new phonon modes below the two-vison continuum. As the vison mass m decreases, these modes move away from the continuum edge and gain spectral weight. For suitable parameters, such modes can be observed by neutron and x-ray scattering at specific momentum. At a critical m, one of the modes condenses, the lattice distorts, and the system enters a valence-bond crystal phase. This is the analog of the spin-Peierls transition in Z_2 liquid.

A. Z_2 gauge theory

The low-energy physics of the Z_2 liquid on a triangular lattice is described by the Z_2 gauge theory on the dual lattice, i.e., the honeycomb lattice.[33,34] Its Hamiltonian is[34]

$$H = -J \sum_{\langle \mathbf{r}_1 \mathbf{r}_2 \rangle} M_{\mathbf{r}_1 \mathbf{r}_2} \sigma^z_{\mathbf{r}_1} \sigma^z_{\mathbf{r}_2} - \Gamma \sum_{\mathbf{r}} \sigma^x_{\mathbf{r}}. \tag{18}$$

Here, $M_{\mathbf{r}_1 \mathbf{r}_2}$ are Z_2 phases arranged such that the flux through each hexagon is -1. $\sigma^z_{\mathbf{r}}$ either creates or destroys a vison at site $\mathbf{r}$.

Following Misguich and Mila,[34] we introduce the hard-core boson representation:

$$\sigma^z_{\mathbf{r}} = b_{\mathbf{r}} + b^\dagger_{\mathbf{r}}, \quad \sigma^x_i = 1 - 2 b^\dagger_{\mathbf{r}} b_{\mathbf{r}}. \tag{19}$$

We anticipate that the excitations are gapped. Consequently, the hard-core property of the bosons can be neglected since the boson density is small at low energy. The theory is then solved by standard techniques since it is quadratic in boson operators. The low-energy quasiparticles are visons.

The vison energy is minimized at four momenta:[33,34] $\mathbf{k}_1 = -\mathbf{k}_3 = (\pi/6, \pi/2)$ and $\mathbf{k}_2 = -\mathbf{k}_4 = (5\pi/6, \pi/2)$. We denote the vison with momentum $\mathbf{k}_\alpha + \mathbf{q}$ as $a_{\alpha,\mathbf{q}}$. The energy of $a_{\alpha,\mathbf{q}}$ is approximately $\omega_{\mathbf{q}} = \sqrt{m^2 + v_b^2 \mathbf{q}^2}$ for small q. The spectrum features agree with the numerical results of Ref. 35. We introduce vison field operators around $\mathbf{k}_\alpha$:

$$\phi_\alpha(\mathbf{r}) = \frac{1}{\sqrt{V}} \sum_{\mathbf{q}} \frac{1}{\sqrt{2\omega_{\mathbf{q}}}} \exp\left(i\mathbf{q} \cdot \mathbf{r} - \frac{q}{\Lambda} \right) a_{\alpha,\mathbf{q}}, \tag{20}$$

where Λ is the momentum cutoff beyond which the lattice details become important. These fields obey Klein-Gordan equations. They capture the low-energy physics of the Z_2 liquid phase.

B. The vison-phonon coupling

The phonons couple to bond operator $\mathbf{S}_i \cdot \mathbf{S}_j$. As was discussed, the bond operator has two effects on a dimer-covering state. The diagonal part measures the dimer density on bond $\langle ij \rangle$, while the off-diagonal part changes the dimer configuration around the plaquette to which bond $\langle ij \rangle$ belongs. Let us focus on the diagonal part first. The off-diagonal part will only change the overall constant in front of the Hamiltonian thanks to the symmetry arguments presented later.

The dimer density on a bond is related to two vison operators: $\mathbf{S}_i \cdot \mathbf{S}_j \sim c_0 M_{\mathbf{r}\mathbf{r}'} \sigma^z_{\mathbf{r}} \sigma^z_{\mathbf{r}'}$ where $\mathbf{r}$ and $\mathbf{r}'$ are the two dual lattice sites adjacent to bond $\langle ij \rangle$. We rewrite $\sigma^z_{\mathbf{r}}$ in terms of $\phi_\alpha(\mathbf{r})$. The general vison-phonon coupling assumes the following form in the continuum limit:

$$H = \int d^d r \sum_{a,l} \sum_{\alpha \geqslant \beta} u_{a,l}(\mathbf{r}) \left[g^{(a,l)}_{\alpha\beta} e^{i(\mathbf{k}_\alpha + \mathbf{k}_\beta)\cdot \mathbf{r}} \phi_\alpha(\mathbf{r}) \phi_\beta(\mathbf{r}) + f^{(a,l)}_{\alpha\beta} e^{-i(\mathbf{k}_\alpha - \mathbf{k}_\beta)\cdot \mathbf{r}} \phi^*_\alpha(\mathbf{r}) \phi_\beta(\mathbf{r}) + \text{H.c.} \right]. \tag{21}$$

Here, a is the sublattice label and $l = x, y$. $g^{(a,l)}_{\alpha\beta}$ and $f^{(a,l)}_{\alpha\beta}$ are coefficients determined from the Z_2 gauge theory. They are listed in the Appendix.

The form of the vison-phonon coupling can also be fixed up to an overall constant by lattice symmetry. To this end, we determine how $\phi_\alpha(\mathbf{r})$ transforms under translation, rotation by $\pi/3$, and reflection around direction $(1/2, \sqrt{3}/2)$. Due to the presence of π flux, we need to accompany the lattice symmetry operations with specific gauge transformations in order to keep the Hamiltonian intact. These are projective symmetry operations. On a triangular lattice, they were studied by Moessner and Sondi.[29] We follow their convention.

We also determined how the phonon transforms under the same set of lattice symmetry operations. The Hamiltonian is determined by finding the scalar representation of lattice symmetries involving one phonon and two visons. The result agrees with the form obtained from Z_2 gauge theory. This confirms the validity of derived Eq. (21).

C. New phonon modes and the Spin-Peierls transition

We begin to explore the physical consequence of vison-phonon coupling by studying a toy problem. Consider a real scalar field $u(\mathbf{r})$ (phonon) coupled to a complex scalar field $\phi[(r)]$ (vison). The noninteracting Lagrangian reads

$$L = \int d^2\mathbf{r} \left[\frac{1}{2}(\dot{u}^2 - \omega_0^2 u^2) + |\dot{\phi}|^2 - |\nabla \phi|^2 + m^2 |\phi|^2 \right]. \tag{22}$$

Here, $\phi = \phi_1 + \phi_2^\dagger$ where

$$\phi_\alpha(\mathbf{r}) = \int \frac{d^2q}{(2\pi)^2} \frac{1}{\sqrt{2\omega_\mathbf{q}}} a_{\alpha,\mathbf{q}} \exp(i\mathbf{q}\cdot\mathbf{r}) \tag{23}$$

with $\alpha = 1,2$. The vison-phonon coupling assumes the general form as in Eq. (21). We further assume $\mathbf{k}_2 = -\mathbf{k}_1$ and $g_{11} = g_{22} = g$ for simplicity.

Applying Eq. (5), we compute the dynamical susceptibility at momentum $2\mathbf{k}_1$:

$$\chi(\omega,2\mathbf{k}_1) = \frac{g^2}{2v_b^2\omega\pi}\left[\tanh^{-1}\left(\frac{2\sqrt{m^2+v_b^2\Lambda^2}}{\omega}\right) - \tanh^{-1}\left(\frac{2m}{\omega}\right)\right]. \tag{24}$$

Here, Λ is a momentum cutoff. We assume $v_b\Lambda \gg m$. Consider $\omega = 2m - x$ with $0 < x \ll 2m$; the dynamical susceptibility can be approximated by the following expression:

$$\chi(\omega,2\mathbf{k}_1) \approx \frac{g^2}{8v_b^2 m\pi} \log\left(\frac{x}{4m}\right). \tag{25}$$

As $x \to 0^+$, $\chi(\omega,\mathbf{k}_1)$ diverges logarithmically. Such divergence introduces a new phonon mode below $2m$. To make it explicit, we write out the full phonon Green's function under the RPA approximation,

$$G(2m-x,2\mathbf{k}_1) \approx \frac{1}{4m^2 - \omega_0^2 - \frac{g^2}{8\pi v_b^2 m}\log\left(\frac{x}{4m}\right) + i\epsilon}, \tag{26}$$

where ϵ is a small positive number. A pole always exists for small enough x:

$$\frac{x_0}{2m} = 2\exp\left[-\frac{8\pi v_b^2 m(\omega_0^2 - 4m^2)}{g^2}\right]. \tag{27}$$

As m become smaller, the pole is moving away from the lower edge of the two-vison continuum. At a finite critical mass m_c, the new phonon mode condenses and the system enters a valence-bond crystal order. The lattice distorts accordingly. This is the general mechanism of the spin-Peierls transition in Z_2 spin liquid.

The toy model captures the main physical points. For realistic models, there are further technical complications. Consider the triangular lattice; the low-energy vison fields are defined at four different momenta. As a result, new phonon modes are introduced at several locations in momentum space. Also, there are four phonons per unit cell; the dynamical susceptibility is a 4×4 matrix in general. As a result, there could be more than one new phonon mode introduced at a certain momentum.

We want to stress that the possible detection of these new phonon modes paves the way for new dialogues between theory and experiment. Conventional ways to detect nonmagnetic excitations such as specific-heat or thermal-conductivity measurements yield only integrated information. The approach we propose, on the other hand, *predicts* the momentum of the new phonon modes and their relative strength. If such modes are observed with predicted properties, it would provide strong evidence of the existence of Z_2 liquid.

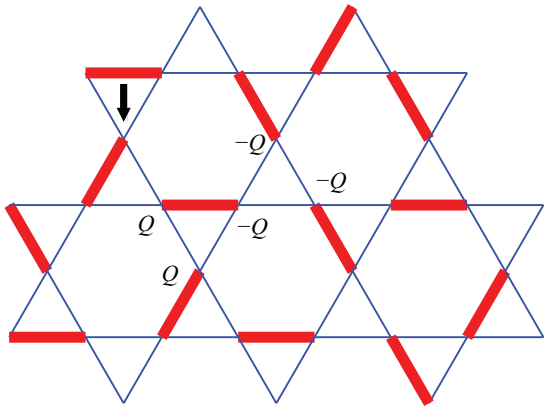

FIG. 3. (Color online) A dimer-covering state of the kagome lattice. A vacuum triangle carries an electric dipole, illustrated by the black arrow, assuming $Q > 0$. Vertices around the defect triangle carry charge $-Q$, while other vertices carry Q.

D. Narrow continuum and bound state of visons

In the previous sections, we assumed that visons behave as free bosons in low energy and that the vison bandwidth is large. These assumptions might not be true on all nonbipartite lattices. For example, it is well known that there is a two-vison bound state at the M point for the quantum dimer model on a triangular lattice around the RK point.[36] For the kagome lattice, the vison dispersion is flat if only the nearest-neighbor interaction is included in the Z_2 gauge theory.[37] If further neighbor interactions are weak, then the two-vison continuum can be very narrow. In both scenarios, two-vison excitations have well-defined energy. Such excitations directly mix with optical phonons and introduce new phonon modes, which can be detected by x-ray or neutron-scattering experiments.

V. POSSIBLE CHARGE SIGNATURE

On nonbipartite lattices, singlet density fluctuations generate electric dipoles.[28] We consider three spins on an equilateral triangle interacting antiferromagnetically. The exchange energy is minimized by combining two of them into a singlet. The induced electric dipole lies in the plane of the triangle normally to the singlet bond[28] (Fig. 3). In other words, charge $2Q$ accumulates on the free spin while the two spins forming the singlet carry charge $-Q$ each. If the dipole is induced by higher-order perturbations in a weak Mott insulator, then $Q > 0$ is proportional to $(t/U)^3$. The sign and the magnitude of spin-lattice coupling determines Q when the dipole is generated by magnetostriction.

Consider a spin-1/2 Heisenberg antiferromagnetic model on the kagome lattice (Fig. 3), i.e., a network of corner-sharing triangles. The low-energy states are dimer-covering states with the maximum number of nearest-neighbor singlets. A quarter of the triangles, the so-called defect triangles, lack singlets.[38,39] The uneven distribution of singlet densities translates into inhomogeneous charge densities. A simple counting shows that the vertices of the defect triangles each carry $-Q$, while all other vertices have Q.

An applied ac electric field can be used to induce the motion of defect triangles. For typical sample size ($L = 1$ mm) and

singlet excitation energy ($\omega = 0.1$ meV), the applied field is approximately uniform, $q = \omega/c \gg 1/L$. The scattering of the applied field will provide information about the singlet spectrum of the system at $\mathbf{q} = 0$. Suitable techniques include, for example, terahertz spectroscopy.

VI. DISCUSSION

In this work, we described how exotic singlet excitations can be detected, at least in principle, by existing spectroscopic methods. While focusing on specific models, we stress that the two mechanisms described are *model independent* as long as the global SU(2) symmetry is intact.

Currently, two classes of materials could host the Z_2 liquid state. The first set of materials, including $ZnCu_3(OH)_6Cl_2$ (herbertsmithite), $Cu_3V_2O_7(OH)_2{\cdot}2H_2O$ (volborithite), and $BaCu_3V_2O_8(OH)_2$ (vesignieite) (see Refs. 1 and 15 for reviews), realize the $S = 1/2$ Heisenberg antiferromagnetic model on the kagome lattice. Yan *et al.*[12] presented some evidence that the ground state of the model is a Z_2 spin liquid. The vison spectrum were studied by several groups.[37,40,41] They identified the location of low-energy singlet excitations in the reciprocal space. Recently, a single-crystal sample of herbertsmithite was synthesized.[42] Measuring the spectral function of phonons in the magnetic energy range (up to a few meV) could reveal novel singlet excitations. It would also be interesting to measure its spectrum at $\mathbf{q} = 0$ using conventional spectroscopies.

The second class of materials, including κ-(BEDT-TTF)$_2$Cu$_2$(CN)$_3$ and EtMe$_3$Sb[Pd(dmit)$_2$]$_2$ (see Ref. 15 for a review), realizes the multispin exchange model on a triangular lattice. Studies[13,14] show that the ground state of the model can be a gapless or a gapped spin liquid for different parameters. The gapped liquid phase resembles the Z_2 liquid phase with a large number of singlet excitations within the spin gap.[13] While κ-(BEDT-TTF)$_2$Cu$_2$(CN)$_3$[43] seems to host the gapless liquid phase, the flexibility of the material family κ-(BEDT-TTF)$_2$X raises the hope that the gapped liquid phase is the ground state for some other member whose singlet excitations can be observed by studying the phonon spectrum.

Beyond quantum magnetism, singlet excitations are believed to be important for other strongly correlated systems such as high-temperature superconductors.[44] We speculate that similar couplings between optical phonons and singlet excitations also exist. It would be very interesting to search for the trace of singlet excitations in the phonon spectrum in these systems.

ACKNOWLEDGMENTS

I acknowledge helpful discussions with Oleg Tchernyshyov, Michel Gingras, Collin Broholm, and Natalia Drichko. Oleg Tchernyshyov is especially thanked for the careful reading and thorough critiques of an early draft. The work is supported by the US Department of Energy, Office of Basic Energy Sciences, Division of Materials Sciences and Engineering under Award No. DE-FG02-08ER46544 and NSERC of Canada.

APPENDIX

In the Appendix, we list $g^{(a,l)}_{\alpha\beta}$ and $f^{(a,l)}_{\alpha\beta}$ derived from the Z_2 gauge theory presented in Sec. IV A. We also checked that these coefficients are fixed up to an overall constant by symmetry. Only nonzero coefficients are listed.

We begin with $g^{(A,l)}_{\alpha\beta}$:

$$g^{(A,x)}_{11} = g^{(A,x)}_{44} = \frac{2}{3}\exp\left(-\frac{2\pi i}{3}\right), \tag{A1a}$$

$$g^{(A,x)}_{22} = g^{(A,x)}_{33} = \frac{2}{3}\exp\left(\frac{2\pi i}{3}\right), \tag{A1b}$$

$$g^{(A,x)}_{12} = g^{(A,x)}_{34} = -\sqrt{\frac{3}{2}}, \tag{A1c}$$

$$g^{(A,x)}_{14} = \frac{2\sqrt{2}}{3}\exp\left(\frac{5\pi i}{6}\right), \tag{A1d}$$

$$g^{(A,x)}_{23} = \frac{2\sqrt{2}}{3}\exp\left(-\frac{5\pi i}{6}\right), \tag{A1e}$$

$$g^{(A,y)}_{11} = -g^{(A,y)}_{44} = \frac{2\sqrt{3}}{3}\exp\left(-\frac{\pi i}{6}\right), \tag{A1f}$$

$$g^{(A,y)}_{22} = -g^{(A,y)}_{33} = -\frac{2\sqrt{3}}{3}\exp\left(\frac{\pi i}{6}\right), \tag{A1g}$$

$$g^{(A,y)}_{13} = -g^{(A,y)}_{24} = 1, \tag{A1h}$$

$$g^{(A,y)}_{12} = -g^{(A,y)}_{34} = -\frac{\sqrt{2}i}{2}. \tag{A1i}$$

$g^{(B,l)}_{\alpha\beta}$:

$$g^{(B,x)}_{11} = -g^{(B,x)}_{44} = g^{(B,x)}_{22} = -g^{(B,x)}_{33} = \frac{2i}{3}, \tag{A2a}$$

$$g^{(B,x)}_{12} = -g^{(B,x)}_{34} = \sqrt{\frac{3}{2}}i, \tag{A2b}$$

$$g^{(B,x)}_{14} = -g^{(B,x)}_{23} = \frac{2\sqrt{2}}{3}i, \tag{A2c}$$

$$g^{(B,y)}_{11} = g^{(B,y)}_{44} = g^{(B,y)}_{22} = g^{(B,y)}_{33} = \frac{2\sqrt{3}}{3}, \tag{A2d}$$

$$g^{(B,y)}_{13} = -g^{(B,y)}_{24} = -1, \tag{A2e}$$

$$g^{(B,y)}_{12} = g^{(B,y)}_{34} = \frac{1}{\sqrt{2}}. \tag{A2f}$$

$f^{(A,l)}_{\alpha\beta}$:

$$f^{(A,x)}_{12} = \frac{2\sqrt{2}}{3}\exp\left(\frac{5\pi i}{6}\right), \tag{A3a}$$

$$f^{(A,x)}_{34} = \frac{2\sqrt{2}}{3}\exp\left(-\frac{5\pi i}{6}\right), \tag{A3b}$$

$$f^{(A,x)}_{13} = \frac{2}{3}\exp\left(-\frac{2\pi i}{3}\right), \tag{A3c}$$

$$f^{(A,x)}_{24} = \frac{2}{3}\exp\left(\frac{2\pi i}{3}\right), \tag{A3d}$$

$$f^{(A,x)}_{14} = f^{(A,x)}_{23} = -\sqrt{\frac{3}{2}}, \tag{A3e}$$

$$f^{(A,y)}_{11} = -f^{(A,y)}_{33} = -f^{(A,y)}_{22} = -f^{(A,y)}_{44} = 1, \tag{A3f}$$

$$f_{13}^{(A,y)} = \frac{2\sqrt{3}}{3}\exp\left(-\frac{\pi i}{6}\right), \tag{A3g}$$

$$f_{24}^{(A,y)} = \frac{2\sqrt{3}}{3}\exp\left(-\frac{5\pi i}{6}\right), \tag{A3h}$$

$$f_{14}^{(A,y)} = f_{23}^{(A,y)} = -\frac{\sqrt{2}i}{2}. \tag{A3i}$$

$f_{\alpha\beta}^{(B,l)}$:

$$f_{12}^{(B,x)} = -f_{34}^{(B,x)} = \frac{2\sqrt{2}i}{3}, \tag{A4a}$$

$$f_{13}^{(B,x)} = f_{24}^{(B,x)} = \frac{2i}{3}, \tag{A4b}$$

$$f_{14}^{(B,x)} = f_{23}^{(B,x)} = \sqrt{\frac{3}{2}}i, \tag{A4c}$$

$$f_{11}^{(B,y)} = -f_{22}^{(B,y)} = f_{33}^{(B,y)} = -f_{44}^{(B,y)} = -1, \tag{A4d}$$

$$f_{13}^{(B,y)} = f_{24}^{(B,y)} = \frac{2\sqrt{3}}{3}, \tag{A4e}$$

$$f_{14}^{(B,y)} = f_{23}^{(B,y)} = \frac{1}{\sqrt{2}}. \tag{A4f}$$

[1] *Introduction to Frustrated Magnetism*, edited by C. Lacroix, P. Mendels, and F. Mila (Springer, New York, 2011), Chaps. 2 and 17.
[2] T. Han and Y. Lee, private communication.
[3] Z. Hao and O. Tchernyshyov, Phys. Rev. B **81**, 214445 (2010).
[4] P. Anderson, Mater. Res. Bull. **8**, 153 (1973).
[5] R. Moessner and S. L. Sondhi, Phys. Rev. B **68**, 184512 (2003).
[6] N. Read and B. Chakraborty, Phys. Rev. B **40**, 7133 (1989).
[7] T. Senthil and M. P. A. Fisher, Phys. Rev. B **62**, 7850 (2000).
[8] D. A. Ivanov, Phys. Rev. B **70**, 094430 (2004).
[9] A. Ralko, M. Ferrero, F. Becca, D. Ivanov, and F. Mila, Phys. Rev. B **71**, 224109 (2005).
[10] K. S. Raman, R. Moessner, and S. L. Sondhi, Phys. Rev. B **72**, 064413 (2005).
[11] A. Seidel, Phys. Rev. B **80**, 165131 (2009).
[12] S. Yan, D. A. Huse, and S. R. White, Science **332**, 1173 (2011).
[13] G. Misguich, C. Lhuillier, B. Bernu, and C. Waldtmann, Phys. Rev. B **60**, 1064 (1999).
[14] O. I. Motrunich, Phys. Rev. B **72**, 045105 (2005).
[15] L. Balents, Nature (London) **464**, 199 (2010).
[16] E. Pytte, Phys. Rev. B **10**, 4637 (1974).
[17] J. W. Bray, H. R. Hart, L. V. Interrante, I. S. Jacobs, J. S. Kasper, G. D. Watkins, S. H. Wee, and J. C. Bonner, Phys. Rev. Lett. **35**, 744 (1975).
[18] I. S. Jacobs, J. W. Bray, H. R. Hart, L. V. Interrante, J. S. Kasper, G. D. Watkins, D. E. Prober, and J. C. Bonner, Phys. Rev. B **14**, 3036 (1976).
[19] M. C. Cross and D. S. Fisher, Phys. Rev. B **19**, 402 (1979).
[20] O. Tchernyshyov, R. Moessner, and S. L. Sondhi, Phys. Rev. Lett. **88**, 067203 (2002).
[21] O. Tchernyshyov, R. Moessner, and S. L. Sondhi, Phys. Rev. B **66**, 064403 (2002).
[22] A. B. Sushkov, O. Tchernyshyov, W. Ratcliff II, S. W. Cheong, and H. D. Drew, Phys. Rev. Lett. **94**, 137202 (2005).
[23] T. Rudolf, C. Kant, F. Mayr, and A. Loidl, Phys. Rev. B **77**, 024421 (2008).
[24] F. Wang and A. Vishwanath, Phys. Rev. Lett. **100**, 077201 (2008).
[25] R. Citro, E. Orignac, and T. Giamarchi, Phys. Rev. B **72**, 024434 (2005).
[26] M. Hase, I. Terasaki, and K. Uchinokura, Phys. Rev. Lett. **70**, 3651 (1993).
[27] J. P. Boucher and L. P. Regnault, J. Phys. I (France) **6**, 1939 (1996).
[28] L. N. Bulaevskii, C. D. Batista, M. V. Mostovoy, and D. I. Khomskii, Phys. Rev. B **78**, 024402 (2008).
[29] R. Moessner and S. L. Sondhi, Phys. Rev. B **63**, 224401 (2001).
[30] D. A. Huse, W. Krauth, R. Moessner, and S. L. Sondhi, Phys. Rev. Lett. **91**, 167004 (2003).
[31] See Supplemental Material at http://link.aps.org/supplemental/10.1103/PhysRevB.85.174432.
[32] D. S. Rokhsar and S. A. Kivelson, Phys. Rev. Lett. **61**, 2376 (1988).
[33] R. Moessner and S. L. Sondhi, Phys. Rev. Lett. **86**, 1881 (2001).
[34] G. Misguich and F. Mila, Phys. Rev. B **77**, 134421 (2008).
[35] A. Ralko, M. Ferrero, F. Becca, D. Ivanov, and F. Mila, Phys. Rev. B **76**, 140404 (2007).
[36] A. M. Lauchli, S. Capponi, and F. F. Assaad, J. Stat. Mech. (2008) P01010.
[37] Y. Huh, M. Punk, and S. Sachdev, Phys. Rev. B **84**, 094419 (2011).
[38] V. Elser and C. Zeng, Phys. Rev. B **48**, 13647 (1993).
[39] Z. Hao and O. Tchernyshyov, Phys. Rev. Lett. **103**, 187203 (2009).
[40] P. Nikolic and T. Senthil, Phys. Rev. B **68**, 214415 (2003).
[41] K. Sengupta, S. V. Isakov, and Y. B. Kim, Phys. Rev. B **73**, 245103 (2006).
[42] T. H. Han, J. S. Helton, S. Chu, A. Prodi, D. K. Singh, C. Mazzoli, P. Müller, D. G. Nocera, and Y. S. Lee, Phys. Rev. B **83**, 100402 (2011).
[43] Y. Shimizu, K. Miyagawa, K. Kanoda, M. Maesato, and G. Saito, Phys. Rev. Lett. **91**, 107001 (2003).
[44] P. A. Lee, N. Nagaosa, and X.-G. Wen, Rev. Mod. Phys. **78**, 17 (2006).